



CHORUS

This is the accepted manuscript made available via CHORUS. The article has been published as:

Emergent Rotational Symmetries in Disordered Magnetic Domain Patterns

Run Su, Keoki A. Seu, Daniel Parks, Jimmy J. Kan, Eric E. Fullerton, Sujoy Roy, and Stephen D. Kevan

Phys. Rev. Lett. **107**, 257204 — Published 16 December 2011

DOI: [10.1103/PhysRevLett.107.257204](https://doi.org/10.1103/PhysRevLett.107.257204)

Emergent Rotational Symmetries in Disordered Magnetic Domain Patterns

Run Su,^{1,2} Keoki A. Seu,^{1,2} Daniel Parks,^{1,2} Jimmy J. Kan,³ Eric E. Fullerton,³ Sujoy Roy,¹ and
Stephen D. Kevan^{2,*}

¹Advanced Light Source, Lawrence Berkeley National Laboratory, Berkeley, CA 94720, USA

²Department of Physics, University of Oregon, Eugene, OR 97403, USA

³Electrical and Computer Engineering, University of California, San Diego, CA 92093, USA

Systems with uniaxial anisotropy often form labyrinthine domain structures that exhibit short-range order but are isotropic over a macroscopic length scale. Such a system would not be expected to exhibit precise symmetries. However, their underlying frustration results in a multitude of metastable domain configurations of comparable energy, and driving such a non-equilibrium system externally might be expected to lead to pattern formation. We find that soft x-ray speckle diffraction patterns of the labyrinthine domain structure of a uniaxial CoPd/IrMn magnetic heterostructure reveal a diverse array of hidden rotational symmetries about the magnetization axis, thereby suggesting an unusual form of emergent order in an otherwise disordered system. These symmetries depend sensitively on applied magnetic field, magnetization history, and scattering wave vector. Maps of rotational symmetry as a function of these variables exhibit intriguing structures that can be controlled by manipulating the applied magnetic field in concert with the exchange bias condition.

PACS: 42.30.Ms 78.70.Ck 75.70.Kw 75.60.-d

Corresponding author; email kevan@uoregon.edu

Complex pattern formation is ubiquitous in nature, particularly for materials near a phase boundary or under non-equilibrium conditions.[1-3] For example, it is possible to generate patterns that have varying degrees of translational and rotational order on an isotropic liquid surface.[4] Even a nominally disordered and spatially chaotic glass is not devoid of local order.[5-7] Uniaxial magnetic thin films will often exhibit a labyrinthine domain state [8] with a complex, worm-like topology that results from competing anisotropy, exchange, dipolar, and strain field energies. In this Letter, we present coherent soft x-ray scattering results demonstrating that such nominally disordered domain labyrinths can exhibit emergent rotational symmetries in the space spanned by scattering wave vector, q . The symmetries are often of high, non-crystalline order and reflect an intriguingly complex underlying spatial pattern that forms as the film is driven with an external magnetic field. It is plausible that field-induced changes in hidden rotational symmetries we observe are closely related to Barkhausen cascades, which exhibit behaviors suggesting statistical self-similarity.[9] We speculate that such q -space patterns might be a common feature of a diverse array of complex, domain-forming materials.

Here we explore the hidden rotational domain symmetry in a CoPd/IrMn multilayer with perpendicular magnetic anisotropy that is interleaved by antiferromagnetic IrMn layers so that the domain structure can be modified both by an applied magnetic field and by exchange-bias interactions. The films were grown by dc magnetron sputtering at room temperature with 3 mTorr Ar sputtering pressure. The structure of the multilayer is Ta(3 nm)/Pd(3 nm)/[IrMn(1.8nm)/[Co(0.5 nm)/Pd(0.7 nm)₄]₁₀/Ta(3 nm). The substrate is a smooth, low-stress silicon nitride membrane 150 nm thick and 0.5 mm square. The thickness of layers and stacking order were optimized to obtain perpendicular magnetic anisotropy and to set the antiferromagnetic blocking temperature. The sample was rotated during deposition to avoid any

in-plane orientation induced by the growth. The layers are (111) textured out-of-plane but are polycrystalline in the film plane. The multilayer exhibits perpendicular magnetic anisotropy and a negative exchange bias of 0.06 T when field-cooled (FC) to 100 K, as shown in the magnetization loop in Fig. 1(b). Also shown is the loop above the blocking temperature $T_B = 275$ K, where the bias disappears.

Coherent soft x-ray scattering experiments were performed at beamline 12.0.2.2 at the Advanced Light Source at Lawrence Berkeley National Laboratory in transmission through the sample. An *in situ* magnetic field up to $H = 0.6$ T can be applied normal to the film plane so that the entire field dependence of the magnetic scattering can be probed. The incident photon energy is tuned to the Co L_3 edge at 778.1 eV to maximize the magnetic x-ray scattering contrast.[10] The linearly polarized soft x-ray beam is spatially filtered with a 12 μm diameter pinhole and then directed at perpendicular incidence on the magnetic film. The diffuse scattering signal is collected in transmission with a charge coupled device (CCD) detector located 0.63 m downstream of the sample. With linearly polarized x-rays in our geometry, the magnetic scattering can be isolated by subtracting the charge scattering contribution measured at magnetic saturation.[10-12] The measurement is conducted by first saturating the sample in a negative magnetic field, then collecting speckle patterns at various applied fields as we traverse to positive saturation. For the zero-field-cooled (ZFC) exchange-bias studies, the sample is demagnetized first and then cooled to low temperature in zero field, and for FC studies the sample is saturated then cooled with the field still applied. Fig.1(a) shows a speckle diffraction pattern of the CoPd/IrMn multilayer collected near the coercive field, which varies between 0.05 and 0.12T for the lower branch of the loop, depending on bias conditions. The ring of diffuse magnetic scattering centered at wave vector $q^* = 0.02 \text{ nm}^{-1}$ corresponds to an average domain

periodicity of $2\pi/q^* = 314$ nm at this field. The short-range order on the domains can be further characterized by the width of the ring, $\delta q \sim 0.015$ nm⁻¹, in this image, corresponding to a domain correlation length of 420 nm, or only 1-2 domain periods. The diffuse scattering envelope is modulated by high frequency speckle; the average width of this speckle is set by the photon transverse coherence length and is $\delta q_{sp} = 0.001$ nm⁻¹. The average in-plane isotropy of the magnetic domains leads to a diffraction pattern that is also nominally isotropic around the scattering origin. To investigate possible hidden symmetries, we follow an approach developed by Wochner, *et. al.* [13] by calculating the rotational autocorrelation function (ACF) defined as

$$ACF(q, \Delta) = \frac{\langle I(q, \phi) I(q, \phi + \Delta) \rangle_{\phi} - \langle I(q, \phi) \rangle_{\phi}^2}{\langle I(q, \phi) \rangle_{\phi}^2} \quad (1)$$

where $I(q, \phi)$ is the intensity at scattering wave vector q and azimuthal angle ϕ , and Δ is an angular offset defined in Fig. 1(c). The sums are performed over narrow annular regions centered at wave vector q and having a width on the order of several speckles. We have tested this procedure extensively on real and simulated results. Slightly changing the width of the annular regions, for example, does not significantly alter the resulting ACF's. The center of the scattering pattern is determined to an accuracy of one CCD pixel via an iterative process that aligns speckles that have the approximate inversion symmetry discussed below. The full angular ACF of the speckle pattern in Fig. 1(a) at q^* shown in Fig. 1(d) exhibits two basic symmetries: $ACF(q, \Delta) = ACF(q, -\Delta)$, which results from the real-valued nature of $I(q, \phi)$, and $ACF(q, \Delta) \approx ACF(q, \Delta + \pi)$, which results from the dominant absorptive component of the index of refraction near the Co L₃ resonance. The peaks at both $\Delta = 0$ and $\Delta = \pi$ are due to the speckled nature of diffraction patterns and have a q -width equal to δq_{sp} .

Beyond these basic symmetries, the angular ACFs exhibit a remarkable array of hidden

symmetries. Fig. 1(d), for example, shows a clear 4-fold symmetry with an amplitude that is 25% of the speckle peak. Fig. 1(e) shows a decomposition of Fig. 1(d) into cosine Fourier components, and the dominant 4-fold symmetry is clearly visible. A sampling of rotational ACFs under a variety of conditions is displayed in Fig. 1(f). Odd n -fold symmetries are not observed since these are forbidden by the inversion symmetry noted above. 4-fold and 6-fold symmetry are common, but non-allowed crystallographic symmetries such as 8-fold, 14-fold, and higher are regularly observed as well. This panel also exemplifies ACF's with no dominant symmetry (bottom trace), one dominant symmetry (middle traces), and more than one coexisting symmetry (top two traces). The small-amplitude fine structure observed in the ACF's results from the finite number of pixels included the annular regions.[14]

An attractive feature of studying labyrinthine domains in magnetic films is the ease with which they can be driven with an external magnetic field. The typical q - and H - dependence of dominant rotational symmetries is illustrated in Fig. 2, which displays maps of the cosine Fourier amplitude at various scattering wave vectors as the FC sample is driven along the lower branch of the exchange biased loop in Fig. 1(b). A given rotational symmetries is typically observed over a narrow q -range comparable to a single speckle, $\delta q_{symm} \sim 0.001 \text{ nm}^{-1}$. By contrast, a symmetry often persists over a fairly broad field range, particularly near the coercive field where magnetization reversal is associated primarily with smooth domain wall motion rather than abrupt topological changes in the labyrinth.[15] It is not surprising that changes in hidden rotational symmetry are associated primarily with topological changes in the labyrinth, where large Barkhausen cascades are expected, though at present we lack the sensitivity to detect individual Barkhausen cascades.

An important question is whether certain rotational symmetries are preferred, that is, are

they observed more often than others following excursions to magnetic saturation? We collected a series of 50 speckle patterns at $H = 0.128$ T with excursions to magnetic saturation between each image. Fig. 3(a) maps the cosine Fourier amplitudes averaged over all cycles as a function of q for the unbiased room temperature film. While hidden symmetries are observed in many individual images, they are broadly distributed and thus average out in this map. This result indicates that the symmetries do not arise from local structural disorder or microcrystallinity in the film, which might be expected to favor certain specific domain patterns and symmetries and which would be reproducible with cycling.[11] Moreover, the absence of preferred symmetries after averaging many magnetization cycles is equivalent to averaging over many sample locations and therefore confirms the isotropy of the labyrinth at long length scale. This is analogous to the thermally-driven short-range fluctuations observed in a colloidal glass,[13] where the analogous averaging would be over time rather than over field cycle. The diverse array of high-order rotational symmetries we report here represent an emergent symmetry characterized by a length scale ($2\pi/\delta q_{symm}$) that is longer than the coherence length of the short range order in the domain labyrinths ($2\pi/\delta q$) and comparable to the transverse coherence length ($2\pi/\delta q_{sp}$) of our photon beam.

Beyond their relevance to magnetization reversal, it is interesting to consider whether these spontaneous rotational symmetries can be controlled, as is often possible in systems driven out of equilibrium. Exchange bias, in which uncompensated spins in the antiferromagnetic layer do not flip as the field is reversed, but interact via an exchange interaction across the interface with the spins of the ferromagnet, provides one approach to accomplish this. Figs. 3(b) and 3(c) show similar averages as Fig. 3(a) but for the FC and ZFC films, respectively. In these cases, certain symmetries are observed with high probability. For example, the FC sample exhibits a

dominant 6-fold symmetry at $q = 0.014 \text{ nm}^{-1}$ with high probability, while different symmetries – up to 28-fold! - appear with lower probability at other q -values. Apparently the dominant symmetries are favored by a particular spin structure of the antiferromagnetic layer, which can then be transferred to the ferromagnetic layer as the film traverses the magnetization loop. This may be expected for the ZFC sample as the microscopic domain structure is imprinted into the antiferromagnetic layer[16, 17] during the cooling process. It is more surprising that the FC sample is nearly as proficient as the ZFC sample at favoring certain rotational symmetries, though a biased sample (including this one) almost always shows a higher coercive field than that measured above T_B . This is thought to be driven by increased magnetic disorder and domain wall pinning, which would lead to microscopic memory and, apparently, to reproducible domain symmetries (these are Eric's words, so they must be right).[18]

The above results provide a fascinating glimpse into pattern formation in these complex domain structures. As in other driven non-equilibrium systems, it might well be possible to change or control the symmetry of the pattern with a proper external stimulus, as suggested by the exchange bias results. For example, two-fold rotational symmetry can be trivially produced by applying an in-plane field component during magnetization reversal. Possibly other more complex, time dependent field protocols will favor other hidden symmetries and rotational patterns. Labyrinthine domain patterns observed in many other soft, hard, and biological systems having uniaxial anisotropy might well exhibit similar rotational symmetries,[1-3, 8] and it is interesting to speculate whether these symmetries impact the functioning of these materials. Finally, a multitude of other systems exhibit marginal orders that are thought to help determine macroscopic properties. Excellent examples are provided by the spin-, orbital-, and charge-ordered phases observed in transition metal oxides.[19, 20] The rotational symmetries we have

report here are so localized in q -space that they would be difficult to detect with real-space probes directly. Seeking such symmetries in Fourier space and measuring their evolution with temperature, time, and applied field, and current presents some intriguing possibilities to understand the impact of emergent mesoscale order on material properties.

ACKNOWLEDGEMENTS

The work at LBNL including experiment at ALS and computation on Lawrence cluster was supported by the Director, Office of Science, Office of Basic Energy Sciences, of the U.S. Department of Energy under Contract No. DEAC02-05CH11231. The work of R. Su and D. Parks was partially supported by the U.S. Department of Energy, Office of Basic Energy Sciences, Division of Materials Science and Engineering under grant number DE-FG02-11ER46831. Work at UCSD was partially supported by DOE-BES Award # DE-SC0003678. Kim Kisslinger at Brookhaven National Laboratory fabricated the pinhole. Joshua Turner at SLAC National Accelerator Laboratory facilitated the pinhole-making process.

REFERENCES

- [1] J. P. Gollub and J. S. Langer, *Reviews of Modern Physics* **71**, S396 (1999).
- [2] M. Cross and H. Greenside, *Pattern Formation and Dynamics in Nonequilibrium Systems* (Cambridge University Press, New York, 2009).
- [3] M. C. Cross and P. C. Hohenberg, *Reviews of Modern Physics* **65**, 851 (1993).
- [4] B. Christiansen, P. Alstrøm, and M. T. Levinsen, *Physical Review Letters* **68**, 2157 (1992).
- [5] P. S. Salmon, *Nat Mater* **1**, 87 (2002).
- [6] F. Sausset and D. Levine, *Physical Review Letters* **107**, 045501.
- [7] J. D. Martin, S. J. Goettler, N. Fosse, and L. Iton, *Nature* **419**, 381 (2002).
- [8] M. Seul and D. Andelman, *Science* **267**, 476 (1995).
- [9] G. Durin and S. Zapperi, *Phys. Rev. Lett.* **84**, 4705 (2000).
- [10] J. B. Kortright, Sang-Koog Kim, G. P. Denbeaux, G. Zeltzer, K. Takano, and E. E. Fullerton, *Phys. Rev. B* **64**, 092401 (2001).
- [11] M. S. Pierce, C. R. Buechler, L. B. Sorensen, J. J. Turner, S. D. Kevan, E. A. Jagla, J. M. Deutsch, T. Mai, O. Narayan, J. E. Davies, K. Liu, J. Hunter Dunn, K. M. Chesnel, O. Hellwig, E. E. Fullerton, and J. B. Kortright, *Phys. Rev. Lett.* **94**, 017202 (2005).
- [12] M. S. Pierce, R. G. Moore, L. B. Sorensen, S. D. Kevan, O. Hellwig, E. E. Fullerton, and J. B. Kortright, *Phys. Rev. Lett.* **90**, 175502 (2003).
- [13] P. Wochner, C. Gutt, T. Autenrieth, T. Demmer, V. Bugaev, A. Diaz Ortiz, A. Duri, F. Zontone, G. Grübel, and H. Dosch, *Proc. Nat. Acad. Sci* **106**, 11511 (2009).
- [14] J. C. Dainty, *Laser speckle and related phenomena* (Springer-Verlag, Berlin, 1975).
- [15] O. Hellwig, S. Maat, J. B. Kortright, and E. E. Fullerton, *Physical Review B* **65**, 144418 (2002).
- [16] P. Kappenberger, S. Martin, Y. Pellmont, H. J. Hug, J. B. Kortright, O. Hellwig, and E. E. Fullerton, *Phys. Rev. Lett.* **91**, 267202 (2003).
- [17] K. Chesnel, E. E. Fullerton, M. J. Carey, J. B. Kortright, and S. D. Kevan, *Phys. Rev. B* **78**,

132409 (2008).

- [18] I. Schmid, M. A. Marioni, P. Kappenberger, S. Romer, M. Parlinska-Wojtan, H. J. Hug, O. Hellwig, M. J. Carey, and E. E. Fullerton, *Physical Review Letters* **105**, 197201 (2010).
- [19] E. Dagotto, *Nanoscale Phase Separation and Colossal Magnetoresistance* (Springer, Berlin, 2003).
- [20] Y. Kohsaka, C. Taylor, K. Fujita, A. Schmidt, C. Lupien, T. Hanaguri, M. Azuma, M. Takano, H. Eisaki, H. Takagi, S. Uchida, and J. C. Davis, *Science* **315**, 1380 (2007).

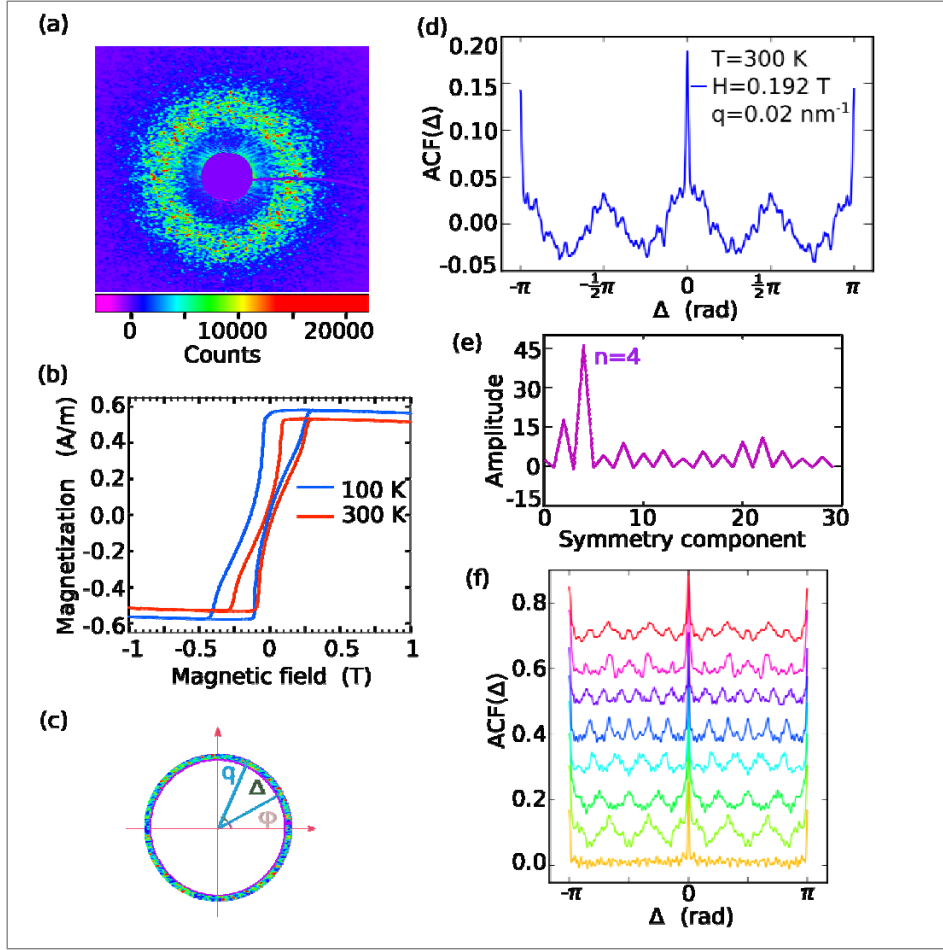


FIG. 1 (color online)(a) Typical speckle diffraction pattern of the labyrinthine domain pattern of the CoPd/IrMn multilayer collected near the coercive field at $T=300$ K. The q -range of this image is $\pm 0.04 \text{ nm}^{-1}$ in both directions. (b) Magnetization loops of the CoPd/IrMn multilayer collected at $T = 300$ K above T_B and at $T = 100$ K below T_B in a FC state. Note the leftward bias of the latter. (c) Annular region of the speckle pattern in panel (a) of nominal radius q in which a rotational autocorrelation pattern is calculated. The angles Δ and ϕ discussed in the text are defined. (d) Rotational autocorrelation function of the annular region in panel (c). (e) Cosine decomposition of the rotational autocorrelation function in panel (d), showing a dominant component at $n = 4$. (f) Collection of several rotational autocorrelation functions that exhibit the diverse hidden symmetries observed.

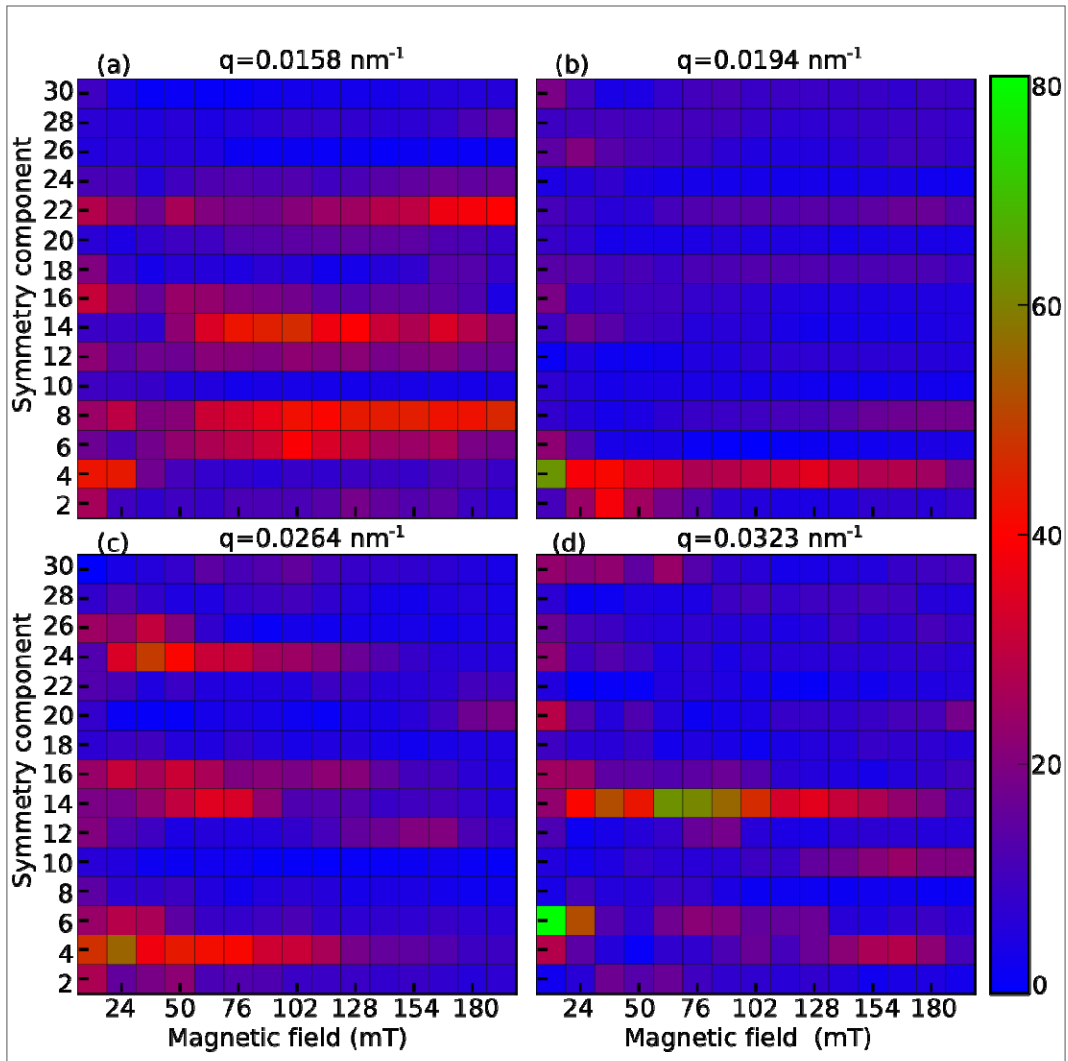


FIG. 2 (color online) Maps of the spectrum of hidden symmetries observed (vertical) as a function of applied field (horizontal) along a single scan along the lower branch of the FC magnetization loop in Fig. 1(b) at values of q (a) below, (b) near, and (c) and (d) above q^* .

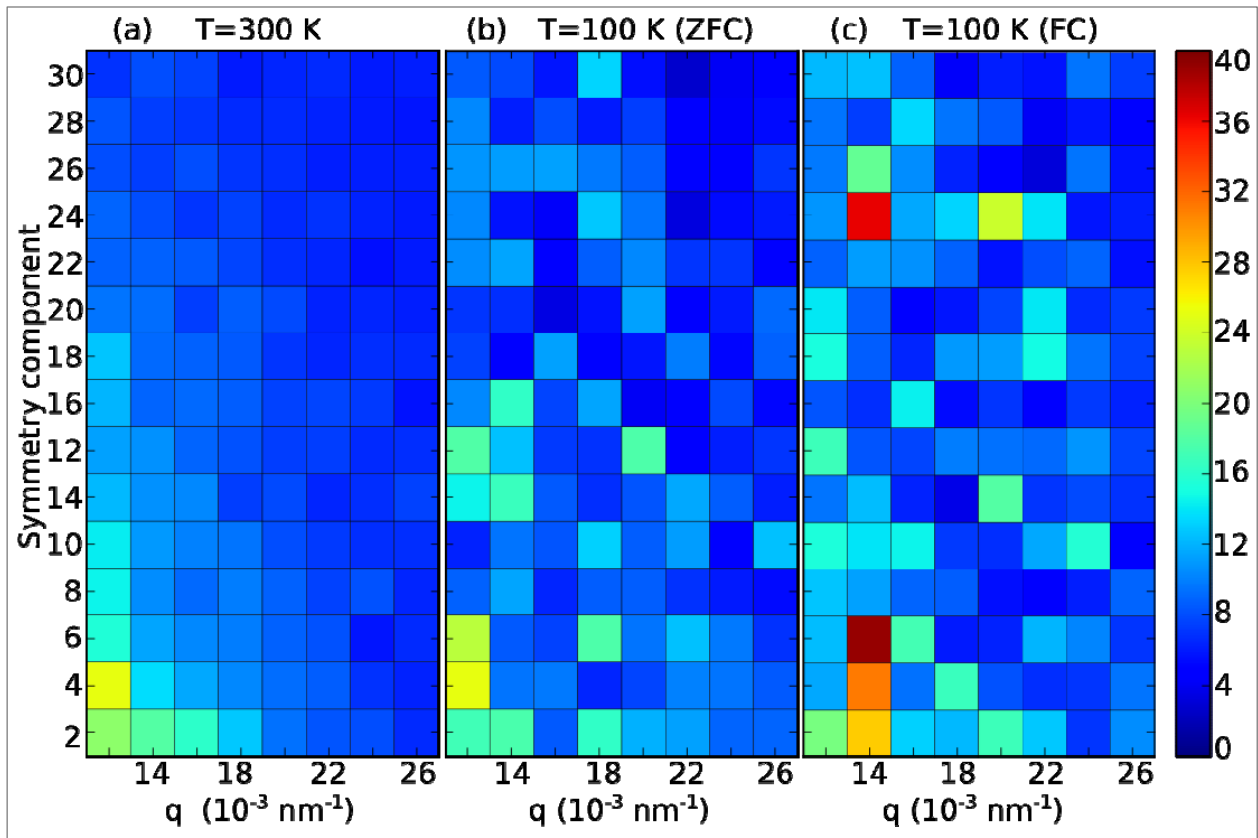


FIG. 3 (color online) Average of 50 cosine decompositions of rotational ACFs symmetry as a function of scattering wave vector collected at $H = 0.128$ T for (a) unbiased (300 K), (b) ZFC, and (c) FC (both 100 K) exchange biased films.